JOURNAL OF MATERIALS SCIENCE 23 (1988) 3509–3514

Particle characterization and cavity nucleation during superplastic deformation in Al–Li-based alloys

M. C. PANDEY
Defence Metallurgical Research Laboratory, Kanchanbagh, Hyderabad 500258, India

J. WADSWORTH
Lockheed Palo Alto Research Laboratory, 3251, Hanover Street, Palo Alto, California 94304, USA

A. K. MUKHERJEE
Division of Materials Science, Department of Mechanical Engineering, University of California, Davis, Calfornia 95616, USA

The role of intermetallic particles on the cavity formation during superplastic deformation has been studied in two aluminium–lithium-based alloys of identical chemical composition. They were, however, manufactured by two different routes – one by ingot metallurgy (IM) and the other by rapid solidification powder metallurgy (PM). A large number of particles of different shapes and sizes were found in both the alloys. In the IM alloy, particles were aligned in stringers in the direction of rolling. Iron and silicon, which were present as impurity elements, formed intermetallic phases in the IM alloy whereas only silicon-rich particles were found in the PM alloy. The particles of the PM alloy were of smaller size and were rather uniformly distributed in comparison to the IM alloy. During superplastic deformation, cavities first nucleated at the interface of large particles. The cavities of the IM alloy formed around the aligned stringers of large particles, whereas in the PM alloy they were uniformly distributed. It is shown that because both alloys contained particles of varying sizes, cavity nucleation occurred continuously during superplastic deformation.

1. Introduction

Failure in superplastic materials often occurs as a consequence of nucleation and growth of grain-boundary cavities. The cavities are usually nucleated at hard particles, grain-boundary triple junctions and at grain-boundary ledges. Several therories have been proposed to explain the mechanism of cavity nucleation during deformation at elevated temperatures [1–5]. According to Ashby [6], a cavity around a particle will nucleate when the local stress concentration becomes appreciably large such that it exceeds the strength of the particle–matrix interface or the fracture strength of the particle. Argon *et al.* [4] calculated the local stress concentration required to induce nucleation of cavities around hard particles in grain boundaries and found it to be 30 to 300 times greater than the applied stress. Fleck *et al.* [2] observed that cavity nucleation occurred as a result of dislocation pile-ups at grain-boundary particles. In superplastic materials, extensive grain-boundary sliding and pile-up of dislocations during deformation can lead to build up of sufficiently large local stresses around particles resulting in cavity nucleation by particle–matrix decohesion process.

In an earlier study on ingot and power metallurgically processed aluminium–lithium-based alloys of almost similar chemical composition, we examined the superplastic deformation behaviour [7], deformation-induced concurrent grain growth [8] and cavitation phenomenon [9]. In both alloys extensive cavitation occurred during superplastic deformation. However, the cavity sizes in the two alloys were found to be different during the initial stage of deformation. In the alloy processed by powder metallurgy process, the size of the cavities in specimens deformed below 200% elongation were found to be smaller in comparison to

TABLE I Chemical compositions of both IM and PM aluminium–lithium-based alloys in weight and atomic per cents

IM		PM	
wt %	at %	wt %	at %
93.95 Al–1.90 Li–2.85 Cu–1.0 Mg–0.15 Zr–0.8 Fe–0.05 Si–0.02 Ti	90.6 Al–7.11 Li–1.16 Cu–1.07 Mg–0.043 Zr–0.0372 Fe–0.046 Si–0.010 Ti	94.1 Al–1.90 Li–2.80 Cu–0.86 Mg–0.2 Zr–0.08 Fe–0.06 Si	90.75 Al–7.11 Li–1.14 Cu–0.92 Mg–0.057 Zr–0.037 Fe–0.055 Si

0022–2461/88 $03.00 + .12

the alloy processed by the ingot metallurgy method [9]. The aim of the present work was to characterize particles and to study their size, shape and role on the formation of cavities during superplastic deformation.

2. Experimental procedure

The chemical composition of the two aluminium–lithium-based alloys, one produced by ingot metallurgy (IM) and the other by rapid solidification powder metallurgy (PM) methods are given in Table I [10]. The IM alloy was prepared by chill casting an ingot of 219 mm diameter, followed by heating in air using a two-stage process consisting of 16 h at 460° C and 16 h at 500° C. The ingot was scalped to 178 mm diameter, and then extruded at 470° C to a bar of rectangular cross-section of 64 mm × 16 mm using an extrusion ratio of 25 : 1. In the case of PM alloy, direct chill-cast remelt stock was converted into powder by centrifugal atomization in helium. The powder was screened in helium to 100 mesh, and subsequently degassed by passing through a vacuum furnace at 538° C for 5 h. This was followed by upsetting, using a blind die and its subsequent extrusion at 382° C into a rectangular bar of cross-section 64 mm × 16 mm with an extrusion ratio of 22 : 1. In order to attain superplastic properties in both alloys, the bars were solution treated at 538° C for 0.5 h followed by cooling in water. Further heating was carried out at 400° C for durations ranging from 0.5 to 136 h. The bars of both alloys were then deformed at 300° C by rolling to a thickness of 1.6 mm (or to a true compressive strain of 2.3).

Tensile specimens (gauge length – 10 mm and width 5 mm) were cut longitudinally in the rolling direction from the 1.6 mm thick sheets. Specimens were tested at true strain rates in the range of 10^{-4} to 10^{-3} sec^{-1} at 450° C in an Instron tensile testing machine which was modified to conduct tests at constant true strain rates. The specimen was preheated to the test temperature in the machine for 0.5 h prior to the commencement of superplastic deformation. The grain size of both the alloys was measured by the linear intercept method after heating for 0.5 h at 450° C. Grain size of the IM and PM alloys were found to be approximately 1 and 0.5 μm, respectively. Tested specimens were polished using conventional polishing techniques. The final polishing was done using 1 μm sized diamond paste in several stages and using ultrasonic cleaning of the specimens between the stages. The polished specimens, both tested and untested, were examined by optical and scanning electron microscopy. Particles of both the alloys were analysed using electron probe micro-analyser (EPMA) having a spot size of 1 μm.

3. Results

3.1. IM alloy

Figs 1a to c show the size and distribution of particles in two samples of the IM alloy heated at 450° C for 1 and 7 h. A large number of particles, as observed in Fig. 1, were also found in the as-received material. It can be observed that particles are aligned in stringers in the direction of rolling and also that there is a wide variation in the particle size. The particles were analysed by EPMA for different elements present in the alloy (Fig. 2). It can be seen that iron and silicon, which were present as impurity elements, had formed intermetallics. In general, the size of the silicon-rich particles was bigger than that of the iron-rich particles. Further, it should be possible to distinguish between the two types of particles by their appearances. The

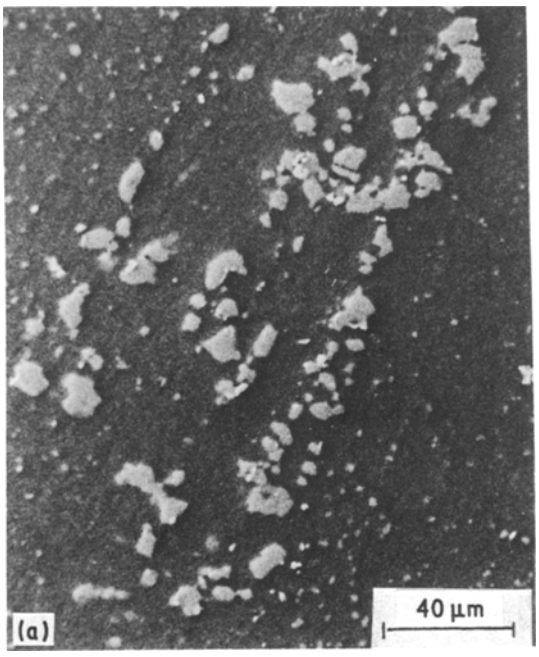

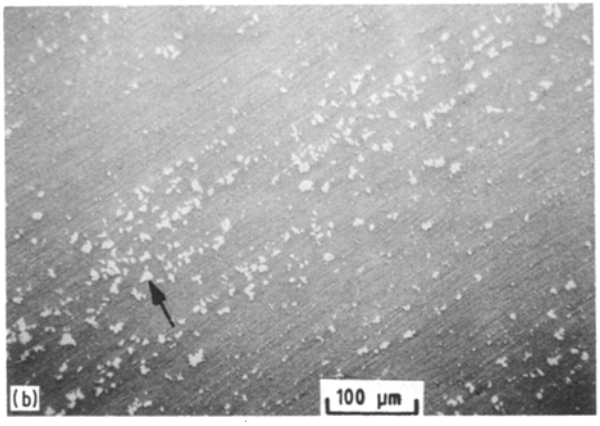

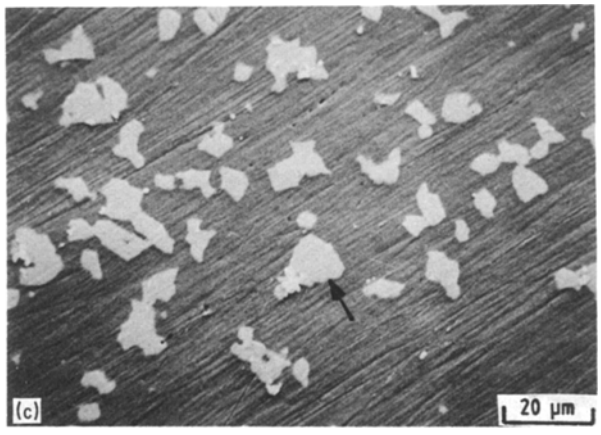

Figure 1 The effect of heating time at 450° C on the size and distribution of particles in the IM alloy, (unetched); (a) 1 h, rolling direction is 80° to the horizontal axis, (b) 7 h, rolling direction is 45° to the horizontal axis. (c) Magnified view of the structure shown in (b).

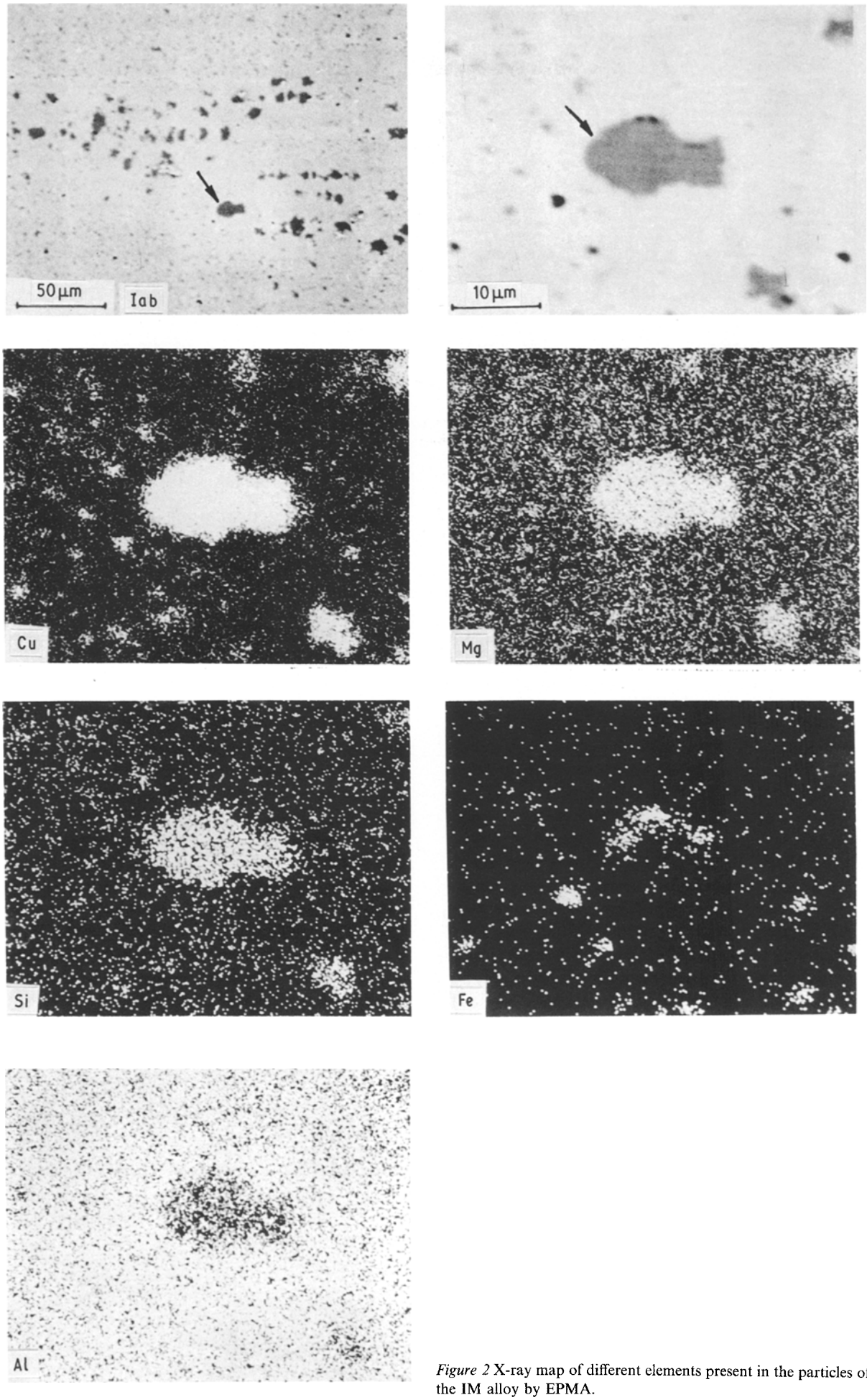

Figure 2 X-ray map of different elements present in the particles of the IM alloy by EPMA.

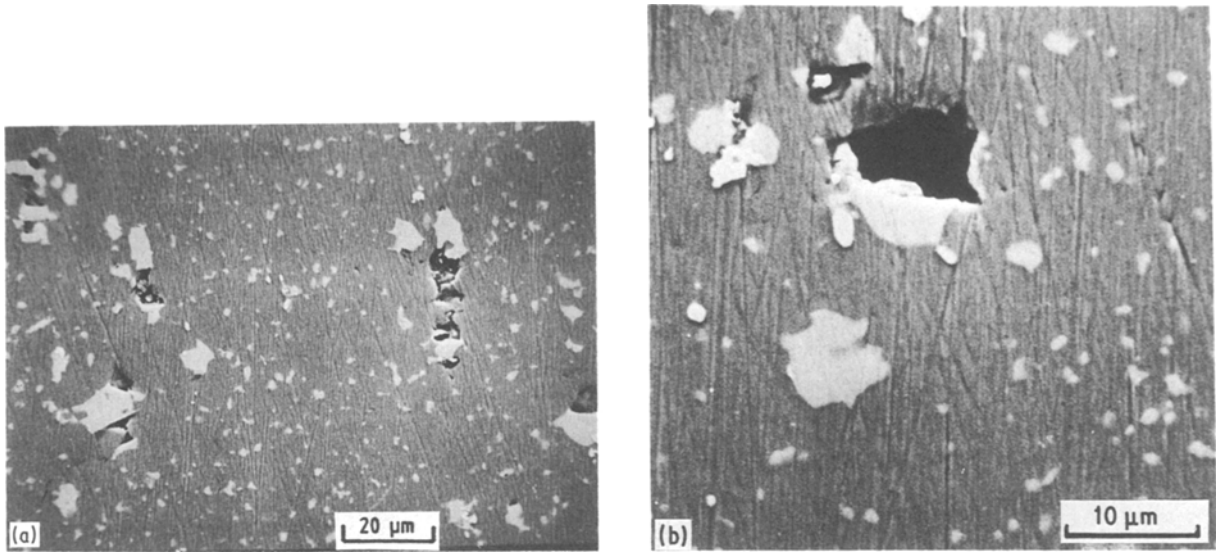

Figure 3 (a) and (b) Scanning electron micrographs of an interrupted specimen of the IM alloy (strain 0.49) tested at a strain rate of 7×10^{-4} sec^{-1} and at 450° C (unetched).

iron-rich particles contained copper and aluminium. Intermetallics such as Al_7Cu_2Fe, $Al_{23}Fe_4Cu$ and Al_9Fe_3Cu have been identified in other Al–Li based alloys [11, 12]. On the other hand, the silicon-rich particles contained magnesium besides aluminium and copper. Lithium in these particles could not be determined due to the limitation of the equipment.

Pandey *et al.* [9] have found extensive cavitation during superplastic deformation of the IM alloy tested at 450° C in the strain-rate range of 10^{-4} to 10^{-3} sec^{-1}. Optical metallography and density measurement of the interrupted specimens have shown that nucleation of cavities occurred during the early stage of superplastic deformation process [9]. Scanning electron microscopy of an interrupted specimen revealed that cavities first nucleated at large particles (Figs 3a and b). Fig. 4 shows cavities formed at particles aligned in stringers in the direction of the stress axis. An example of the cavitation behaviour in a specimen tested to failure is shown in Fig. 5.

3.2. PM alloy

The size and distribution of particles in the PM alloy heated at 450° C for 1 and 7 h are shown in Figs 6a and b. The particles are of different sizes and rather uniformly distributed as compared to the IM alloy. The EPMA study of the alloy revealed that some of the particles contained silicon besides copper, magnesium and aluminium. Iron-rich particles were found to be absent.

Extensive cavitation occurred at all the strain rates (10^{-4} to 10^{-3} sec^{-1}), and cavities nucleated during early stages of superplastic deformation, as also found in the IM alloy [9]. Fig. 7 shows the cavitation behavior (close to the fracture end) of a specimen tested at a strain rate of 2.5×10^{-3} sec^{-1}. It can be noticed that the cavities are of different sizes and they are rather uniformly distributed. Fig. 8 is a scanning electron micrograph showing cavities associated with the particles in a region close to the end of the gauge length of a specimen tested to failure. Microstructural examination at the other end of the gauge length was carried out to establish a link between the particles and cavity nucleating because local deformation was lower than that at the fracture end and therefore the particles were not completely decohesed.

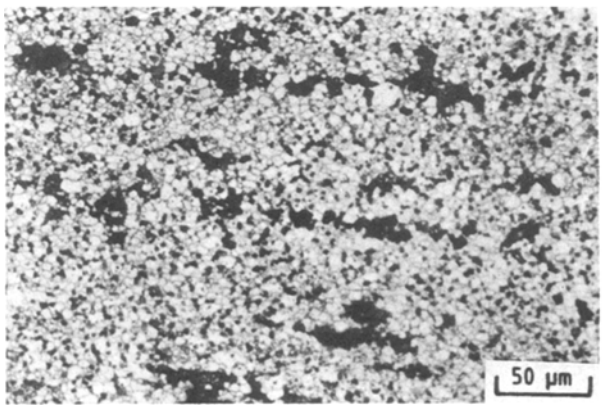

Figure 4 Cavities formed in stringers, following the distribution of particles. Strain rate -2.5×10^{-3} sec^{-1} (etched), stress axis is horizontal.

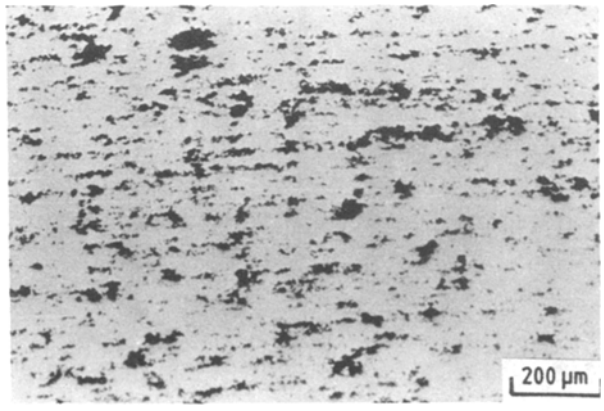

Figure 5 Cavitation in a fractured sample of the IM alloy tested at a strain trate of 2.5×10^{-3} sec^{-1} and at 450° C (strain to fracture 1.65), stress axis is horizontal (specimen unetched).

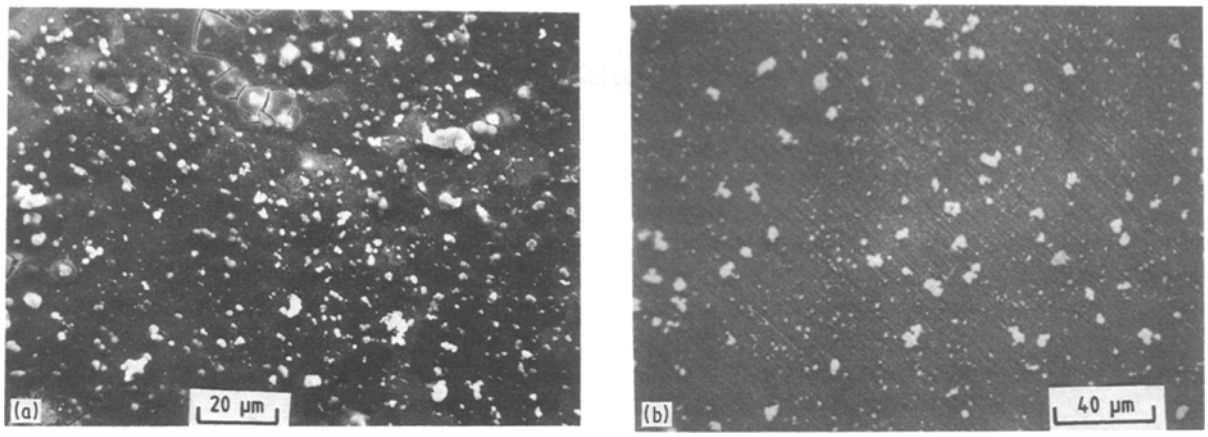

Figure 6 Scanning electron micrographs showing size and distribution of particles in the PM alloy heated at 450° C, (a) 1 h (etched in boiling 90/10 methenol/bromine solution), (b) 7 h (unetched).

4. Discussion

Our investigation has shown that the distribution and size of particles are linked with the manufacturing routes employed. For example, processing by ingot metallurgy route caused particles to align in stringers in the direction of rolling. It has been observed that cavities in the superplastically deformed specimens of the IM alloy also form stringers aligned in the direction of the stress axis, whereas they are uniformly distributed in the PM alloy, illustrating that there is a strong relationship between particle and cavity distribution. Strong evidence that cavities in both the alloys nucleated at the particle interface has been provided by scanning electron microscopy. Similar observations have been made in a superplastic copper alloy wherein particles formed stringers in the direction of rolling and, during superplastic deformation cavities nucleated around these particles [13, 14].

During superplastic deformation cavities first nucleated at the interface of large particles (Fig. 3a). This can be explained as follows: in both the alloys, many particles are 5 to 10 times bigger than the grain size. This means that a large particle may occupy 5 to 10 grains depending on the particle size. Because a large number of grain boundaries are associated with a single particle, extensive grain-boundary sliding during superplastic deformation leads to stress build-up at the particle interface. The larger is the particle size, the greater will be the stress build-up resulting in cavity nucleation first around these particles. Fig. 9 is a schematic diagram showing cavity nucleation at a particle interface due to stress build-up by grain-boundary sliding. In this case, we have shown an extreme example of a particle which has a non-uniform shape, long and thin. Cavities may nucleate either at the particle interface or cracking may take place within the particle or both may occur. If the particles have sharp edges, it may give rise to the notch effect. Cavity nucleation may also depend on the number of grain boundaries impinging on a particle and proportion of the boundaries undergoing sliding.

Cocks [15] has provided theoretical understanding of the mechanism of cavity nucleation in creeping solids. He has argued that if accommodation is by diffusion around a particle, then stress is greatest on the large particles and cavities will nucleate first on them. However, if accommodation is by plastic flow of matrix, then the stress is greatest on the smaller particles and cavities will nucleate first on them instead. This argument of cavity nucleation mechanism holds good also in the case of superplastic materials. The only difference between superplastic materials and creeping solids is that the former has a smaller grain

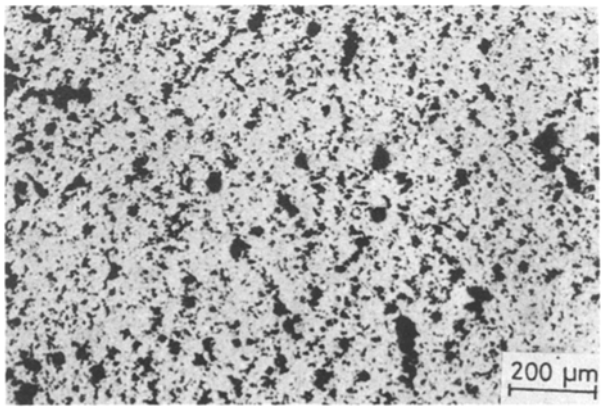

Figure 7 Optical micrograph showing size and distribution of cavities close to the fracture end of a PM alloy specimen (unetched) tested at a strain rate of 2.5×10^{-3} sec^{-1} and at 450° C (strain to fracture 1.56). Stress axis is horizontal.

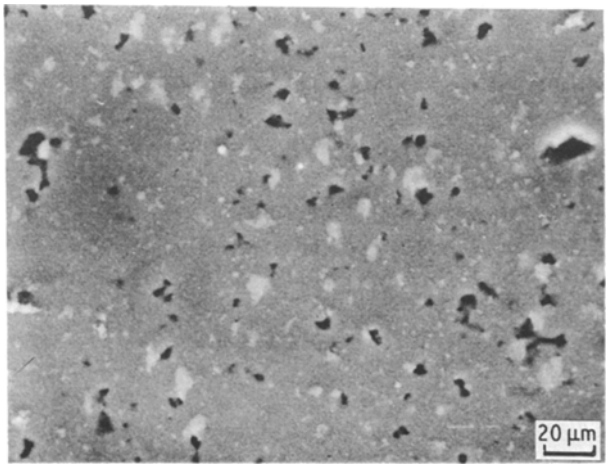

Figure 8 Scanning micrograph was taken at the end of the gauge length of a specimen in order to show that the cavities are associated with the particles. Testing details as given in Fig. 7.

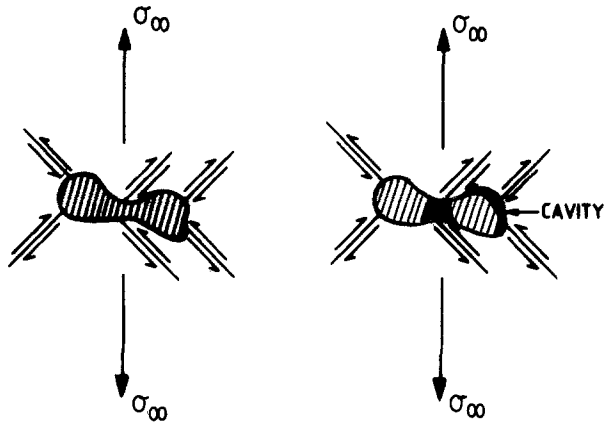

Figure 9 Schematic diagram showing cavity formation at the periphery as well as in the middle of the particle due to stress build up caused by grain boundary sliding.

size and the particles can occupy more than one grain boundary depending upon the particle size. In the case of superplasticity, the primary mode of deformation is widely accepted to be that of grain-boundary sliding and the accommodation process is normally considered to be diffusional one. According to the argument presented above, cavities should then first nucleate at the interface of large particles. Once cavities have nucleated atoms diffuse out from the nucleated sites and may deposit around neighbouring particles, therby increasing the possibility of cavity nucleating in remaining particles. This illustrates that cavity nucleation occurs continuously during superplastic deformation and the wide variation in the cavity size in the fractured specimens of both alloys (Figs 5 and 7) confirms this.

5. Conclusions

1. Particles of varying sizes were found in both IM and PM alloys. In the IM alloy, the particles formed stringers in the direction of rolling whereas in the PM alloy they were rather uniformly distributed and were of smaller sizes.

2. Iron and silicon, present as impurities, formed intermetallics. Magnesium was found to be absent in the iron-rich particles which were of considerably smaller size than the silicon-rich particles. In the case of PM alloy, iron-rich particles were found to be absent.

3. Cavities first nucleated at the interface of large particles. In the IM alloy, cavities formed in stringers in the direction of the stress axis whereas they were rather uniformly distributed in the PM alloy. There is circumstantial evidence that cavities continuously nucleated during superplastic deformation.

Acknowledgements

The research was supported by the US Air Force Office for Scientific Research and the Lockheed Independent Research Programme while MCP was a Post Doctoral Fellow at the University of California. We would like to thank Professor P. Rama Rao, Director, DMRL for the provision of facilities at DMRL.

References

1. J. E. HARRIS, *Trans. AIME* **233** (1965) 1509.
2. R. G. FLECK, D. M. R. TAPLIN and C. J. WEAVERS, *Acta Metall.* **23** (1975) 415.
3. R. RAJ and M. F. ASHBY, *ibid.* **23** (1975) 653.
4. A. S. ARGON, I. W. CHEN and C. W. LAU, in "Creep-Fatigue-Environment Interactions", edited by R. M. Pelloux and N. S. Stoloff (Metallurgical Society of AIME, Warrendale, Pennsylvania, 1980) p. 46.
5. A. J. PERRY, *J. Mater. Sci.* **9** (1974) 1016.
6. M. F. ASHBY, *Phil. Mag.* **14** (1966) 1157.
7. M. C. PANDEY, J. WADSWORTH and A. K. MUKHERJEE, *Mater. Sci. Engr.* **80** (1986) 169.
8. M. C. PANDEY, J. WADSWORTH and A. K. MUKHERJEE, *Scripta Metall.* **20** (1985) 2661.
9. M. C. PANDEY, J. WARDSWORTH and A. K. MUKHERJEE, *Mater. Sci. Engr.* **78** (1986) 115.
10. J. WADSWORTH, I. G. PALMER, D. D. CROOKS and R. E. LEWIS, in "Superplastic Behaviour of Al–Li Alloys", Proceedings of the Second International Al–Li Conference, edited by E. A. Starke and T. H. Sanders (Metallurgical Society of AIME, Warrendale, Pennsylvania, 1983) pp. 111–36.
11. N. J. OWEN, D. J. FIELD and E. P. BUTLER, *Mater. Sci. Technol.* **2** (1986) 1217.
12. R. J. KAR, J. W. BOHLEN and G. R. CHANANI, in "Superplastic Behaviour of Al–Li Alloys", Proceedings of the Second International Al–Li Conference, edited by E. A. Starke and T. H. Sanders (Metallurgical Society of AIME, Warrendale, Pennsylvania, 1983) p. 255.
13. C. H. CACERS and D. S. WILKINSON, *Acta Metall.* **32** (1984) 423.
14. A. CHOKSI, *Metall. Trans. A* **18A** (1987) 63.
15. A. C. F. COCKS, *Acta Metall.* **33** (1985) 129.

Received 15 October 1987
and accepted 11 February 1988